Vision, Modeling, and Visualization (2011)
Peter Eisert, Konrad Polthier, and Joachim Hornegger (Eds.)

Landmark-constrained 3-D Histological Imaging: A Morphology-preserving Approach

S. Gaffling[1,2] and V.Daum[1] and J.Hornegger[1,2]

[1]Pattern Recognition Lab, Friedrich-Alexander-Universität Erlangen-Nürnberg, Germany
[2]School of Advanced Optical Technologies (SAOT), Friedrich-Alexander-Universität Erlangen-Nürnberg, Germany

Abstract

The inspection of histological image sequences to gain knowledge about the original three-dimensional (3-D) morphological structure is a standard method in medical research. Its main advantage is that light microscopes feature high resolution enhanced visibility due to staining. In many cases this imaging technology could immensely profit from 3-D reconstructions of the slice images. For volumetric stacking, however, the tissue deformations due to slice preparation require an unwarping strategy to restore the original morphology. The challenge is to reverse the artificial deformations while preserving the natural morphological changes. In particular, unintentional straightening of curved structures across multiple slices has to be avoided. In this article, we propose a novel way to incorporate landmarks representing the morphological progression. They are used as additional regularization for intensity based non-rigid registration which is capable to exactly match the landmarks. Our approach is tested on synthetical and histological data sets. We show that it delivers smooth contours while preserving the morphological structure, and is a promising addition to existing methods.

Categories and Subject Descriptors (according to ACM CCS): I.4.3 [Image Processing and Computer Vision]: Enhancement—Registration, Geometric Correction

1. Introduction

The investigation of histological image sequences is an everyday task in biomedical laboratories. Conventional light microscopes have a high resolution of up to 0.5 μm, and the possibility to stain structures of interest beforehand enhances visibility and perception. Imaging modalities that are able to directly visualize 3-D objects, e.g., μ-CTs, only recently achieve similar values with about 0.7μm, but without the benefits tissue staining offers.

The main drawback of histological imaging, however, is that the spatial connection of structures is lost during cutting. This is especially a disadvantage when the progression of anatomical structures has to be investigated. Mentally recombining the 2-D image sequences then can often be a challenge. Furthermore, biomedical research often requires the extraction of quantitative values, which is usually best and most reliably done using volumetric data.

In these cases, a 3-D reconstruction of the original tissue from the histological image sequence can immensely facilitate the perception of the morphology and spatial information. An important requirement is, that the final reconstruction should restore the anatomy such that it matches its original in vivo tissue sample before it was extracted from the specimen.

However, this is not a straightforward procedure of merely stacking the 2-D images. As tissue preparation and image acquisition create many artifacts such as intensity inhomogeneities, lighting artifacts, differently oriented slices, cuts and tears the reconstruction process requires several processing steps.

Of particular relevance is the severe mechanical stress the tissue samples are subject to during slicing. The resulting deformations prevent a proper reconstruction and perception of the original morphology. These deformations are therefore usually reversed using non-rigid registration methods, a process to find a deformation matching two images of similar content. Such a method can be used to perfectly align

DOI: 10.2312/PE/VMV/VMV11/309-316

morphological structures and enable smooth structure progression.

But, as was in detail explained in [MEBNV04, SMH*07], conventional non-rigid registration of histological image sequences tends to straighten curved structures, which is known as "banana problem" [SWM97], see fig. 1. It is a consequence of the fact that histological image sequences contain both the natural progression of morphological structures, as well as the deformation due to mechanical stress during slicing. While the latter is the actual target of the non-rigid registration, the former should be preserved.

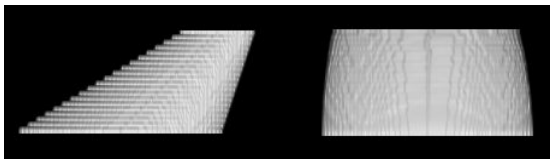

Figure 1: *Detail images of reconstructions using synthetic images. Left: Stacked original slices. Right: Non-rigid registration mostly optimizes overlap and smooth contour progression, but alters original object.*

Related Work

Many different methods were invented for histological image registration, covering a broad range of possible approaches. An extensive overview can be found in [SMH*07]. The most reliable way for smooth but anatomically correct reconstruction is to use ground truth data of the tissue sample. It is often acquired prior to slice preparation, e.g., an MR volume [DDC*07]. External references are however mostly not available. Ju et al. [JWC*06] propose a weighted averaging scheme of deformation fields which were calculated in the neighborhood of the currently considered slice.

The basis for our approach is a non-parametric non-rigid registration scheme that restricts the allowed deformations. As a 2-D translation has to be determined for each pixel, this is generally a highly underdetermined problem. Therefore, a constraining function, called regularizer or smoother, is usually designed to restrict the free-form deformation calculated by the registration method in a certain manner. Two commonly used regularizing strategies are discussed in [Mod03]. One is based on the second derivatives of the deformation field, penalizing strong curvature, and therefore called curvature regularizer. The second one was already applied in histological image reconstruction [SMH*07], and restricts the elastic potential of the deformation.

Landmarks have been used in combination with intensity-based image registration in several ways before. Johnson and Christensen [JC02] alternate between optimization of landmark position and intensity-based registration. Hartkens et al. [HHC*02] and Urschler et al. [UZDB06] add an additional energy term incorporating the landmarks to the objective function. Both approaches take the landmark position into account, but cannot guarantee an exact match in the end. In contrast to that, Fischer et al. [FM03a] incorporate the landmarks as hard constraints into the registration routine, and thus can exactly match the landmarks. The Lagrange multipliers used for this purpose however make the computation more complex the more landmarks are considered.

Goal of this work

Complementary to the above-mentioned methods, we propose to incorporate the morphological structure into the regularization scheme. We first manually extract anatomical landmarks to generate an initial model of the original morphology. This is achieved by performing a polynomial fit of those points that correspond to the same morphological structure. In this way, smooth trajectories are fitted through the entire volume. The offset of the landmarks to the trajectory then serves as initial sparse deformation field to a curvature-regularized non-rigid registration scheme. The capability of the registration scheme to exactly position landmarks, combined with the correction of prominent anatomical structures to their approximated original location on the trajectories offers new possibilities in anatomically correct histological image reconstruction.

Section 2 first explains the approximation of the morphology by landmarks, and subsequently their use in the non-rigid registration scheme. Results on synthetic and histological data sets are shown in section 3. The proposed method is discussed and the article concluded in section 4.

2. Methods

Different image artifacts have to be corrected prior to non-rigid registration. The first steps are comprised of a correction of image intensities and a rigid registration to roughly align the tissue slices. These steps are however not subject of this work.

2.1. Morphology model

For manual tracking, the first image is displayed for the user to select prominent points as landmarks. These landmarks are subsequently tracked through the image sequence. Landmarks belonging to the same anatomical structure therefore build a trajectory through the volume. It is possible to finish trajectories when structures end as well as add new trajectories throughout the volume.

Biological structures are mostly characterized by smooth curves and gradual progression. As a consequence, the selected landmarks — displaced due to cutting — should actually lie on a smooth line. Therefore, to approximate the original morphology, all landmarks belonging to the same trajectory serve as input for a polynomial fitting procedure. We assume that the deformations are in general small, such

that the overall characteristic progression of the structure in consideration is not entirely changed. For our experiments we used a polynomial of order $M = 4$. The ideal image coordinates $\hat{x}, \hat{y}$ for a given landmark on a slice with z-coordinate $z \in \mathbb{R}$ is then given by

$$y(z) = \mathbf{c}_0 + \mathbf{c}_1 z + \mathbf{c}_2 z^2 + \mathbf{c}_3 z^3 = \begin{pmatrix} \hat{x} \\ \hat{y} \end{pmatrix}$$

where $\mathbf{c}_i = \left(c_{ix}, c_{iy}\right)^T \in \mathbb{R}^2$. As fitting procedure, we use a singular value decomposition scheme as described in [PTVF07] to generate a smooth function approximating the assumed morphological progression. This is a linear least-squares problem of the form

$$\hat{\mathbf{c}} = \underset{\mathbf{c}}{argmin} \parallel \mathbf{Ac} - \mathbf{b} \parallel_2^2$$

with $\mathbf{A}$ being the design matrix and $\mathbf{b}$ a vector both derived from the landmarks. $\mathbf{c}$ contains the coefficients $\mathbf{c_i}$ of the polynomial. An example of a fitted trajectory and the landmarks is given in fig.2.

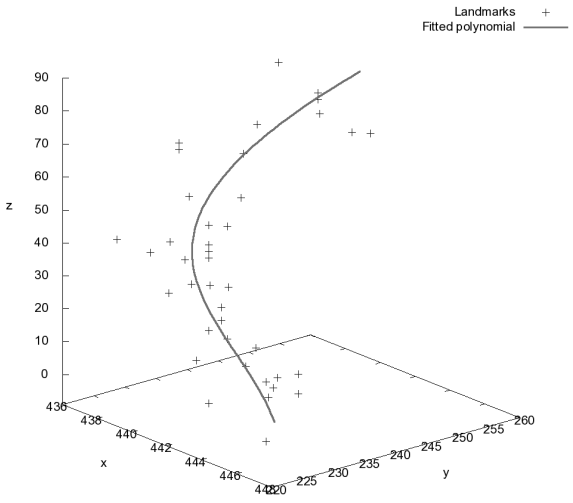

Figure 2: *Landmarks belonging to the same morphological structure, and the fitted trajectory.*

The intersection of the fitted polynomial with the slices gives the estimated true location the respective landmark should lie on. Therefore, a sparse deformation field is created for each slice, indicating for each landmark the offset from its current position to the interpolated new position.

2.2. Non-rigid registration scheme

Non-rigid registration is an essential tool for medical image applications. It can be used to compensate motion between images such that corresponding content is mapped onto each other. In this context we will only provide a brief introduction into the non-rigid, non-parametric registration formulation we use. For a more in-depth discussion please refer to [Mod03].

Mathematically, the aim of a 2-D image registration is to find a mapping $u : \mathbb{R}^2 \mapsto \mathbb{R}^2$ between a reference image R and a template image T, such that the deformed template $T_u(\mathbf{x}) = T(\mathbf{x} - u(\mathbf{x}))$ is similar to R. The similarity of the images is measured by a distance measure $\mathcal{D}$. Additionally we require the deformation u to be regular in some sense, which usually means we want it to be smooth. The smoothness is measured by the regularizer $\mathcal{R}$. All in all, we thus want to solve

$$u^* = \underset{u}{\operatorname{argmin}}\, \mathcal{D}(R, T_u) + \alpha \mathcal{R}(u), \tag{1}$$

where α is a weighting parameter that decides whether we prefer a better match or a smoother deformation. As we only have to deal with mono-modal registration problems in this work we employ the well known sum-of-squared-differences (SSD) as distance measure. It is defined as

$$\mathcal{D}_{\mathrm{SSD}}(R, T_u) = \frac{1}{|\Omega|} \int_\Omega \left(R(\mathbf{x}) - T_u(\mathbf{x})\right)^2 \, \mathrm{d}\mathbf{x}, \tag{2}$$

where Ω is the computational domain of the registration and $|\Omega|$ its area. As regularizer we employ the curvature regularization, popularized in [FM03b]:

$$\mathcal{R}_{\mathrm{CURV}}(u) = \frac{1}{|\Omega|} \int_\Omega \Delta u(\mathbf{x}) \, \mathrm{d}\mathbf{x} \tag{3}$$

Equation (1) is solved by calculating and solving the Euler-Lagrange equations with respect to the unknown function u. In our case this amounts to

$$\left(R(\mathbf{x}) - T_u(\mathbf{x})\right) \nabla T_u(\mathbf{x}) + \alpha \left(\Delta^2 u\right)(\mathbf{x}) = 0 \quad \forall \mathbf{x} \in \Omega \tag{4}$$

In order to actually solve these equations the problem statement has to be discretized. This is done on a cartesian grid $\mathbf{x}$ composed of the grid positions $\mathbf{x}_i$ with $i = 1, \ldots, s$. The deformation u is therefore discretized as the vector $\mathbf{u}$ composed of the 2-D vectors $\mathbf{u}_i = u(\mathbf{x}_i)$. The differential operator Δ^2 is discretized as the matrix $\mathbf{A}$ which can be described by its matrix stencil

$$\frac{1}{h^4} \begin{bmatrix} 0 & 0 & 1 & 0 & 0 \\ 0 & 2 & -8 & 2 & 0 \\ 1 & -8 & 20 & -8 & 1 \\ 0 & 2 & -8 & 2 & 0 \\ 0 & 0 & 1 & 0 & 0 \end{bmatrix}, \tag{5}$$

with h denoting the spacing of the cartesian grid used for the discretization. For the optimization itself we use a semi-implicit gradient descent scheme

$$(\mathbf{I} + \tau\alpha\mathbf{A})\mathbf{u}^{(t+1)} = \mathbf{u}^{(t)} - \tau(R(\mathbf{x}) - T_{\mathbf{u}^{(t)}}(\mathbf{x})) \cdot \nabla T_{\mathbf{u}^{(t)}}(\mathbf{x}). \tag{6}$$

The index t in this context is the iteration index of the non-linear optimization scheme and τ is the step-size parameter.

Into this scheme for a non-rigid registration we now want

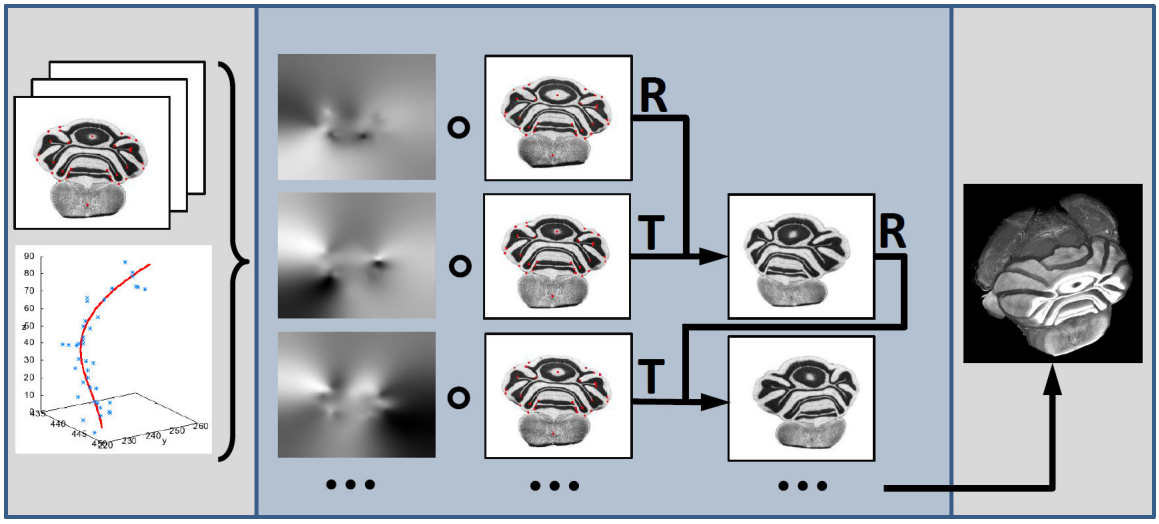

Figure 3: *Overview of the presented workflow.*

to incorporate landmarks. Formally this means that there is an area or a set of areas $\Omega_{\mathbf{p}} \subset \Omega$ with known corresponding locations in the reference image $\mathbf{p}_R$ and the template image $\mathbf{p}_T$. The transformation in these areas is defined as

$$\mathbf{p}_R = \mathbf{p}_T - u(\mathbf{p}_R) \quad \forall \mathbf{p}_R \in \Omega_{\mathbf{p}}. \tag{7}$$

Discretized, this results in a set of corresponding discrete points at locations $\mathbf{x}_i \in \Omega_{\mathbf{p}}$. This was exploited for example by Fischer et al. in [FM03a] by integrating (7) with Lagrange multipliers as constraints into the registration problem. During each iteration step the according Lagrange multipliers have to be determined by solving an additional linear system, whose complexity depends on the number of landmark constraints that are used.

We propose a computationally simpler approach for introducing the landmark constraints in the registration formulation. As the transformation is known in $\Omega_{\mathbf{p}}$, there is, literally, nothing to compute there. We can therefore remove the areas with a known transformation from the computational domain.

$$\tilde{\Omega} := \Omega \setminus \Omega_{\mathbf{p}} \tag{8}$$

The known transformation $u(\mathbf{p}_R) \quad \forall \mathbf{p}_R \in \Omega_{\mathbf{p}}$ is used as a Dirichlet boundary condition. This way the computational work is actually reduced for each constraint that is added, as the computational domain gets smaller and smaller.

In practice, instead of outright eliminating all $\mathbf{u}_i$ corresponding to a landmark location right away we instead replace their rows i in the system matrix $\mathbf{I} + \tau\alpha\mathbf{A}$ by "identity stencils", which, in stencil notation, can be written as

$$\begin{bmatrix} 0 & 0 & 0 \\ 0 & 1 & 0 \\ 0 & 0 & 0 \end{bmatrix}. \tag{9}$$

Additionally, we set the gradient of the distance measure to 0 and therefore the right hand side of (6) to $\mathbf{u}_i^{(t)}$ for these rows. By making these two adjustments it is now ensured that $\mathbf{u}_i$ will not change if one iteration of the non-linear optimization is performed. If $\mathbf{u}^{(0)}$ is initialized with the known transformation from the corresponding point-to-point correspondence, it will stay constant throughout the iteration. The neighborhood of these boundary points, however, will be influenced through the regularizer.

The resulting linear problem that has to be solved during one iteration of the non-linear optimization is not symmetric, but it is positive definite. We therefore employ a stabilized biconjugate gradient method, which can deal with these types of linear problems.

We initialize the deformation $\mathbf{u}^{(0)}$ with the already known offset of the landmarks to the trajectories. This sparse deformation field is then transformed into a dense deformation field by solving just for the regularizer with its boundary conditions, by means of a direct sparse matrix solver. The sparse matrix solver is applied on a downsampled representation of the problem due to memory constraints. This good initialization allows us to use fewer iterations of the iterative method in the registration scheme and thus to speed up the computation.

2.3. Volume reconstruction

The reconstruction result mainly depends on the type of non-rigid registration. However, the manner in which the registration is applied to the entire image sequence also influences the volume quality. There are different strategies that can be applied, for example calculating a weighted average of deformation fields in the neighborhood of a current slice, or

iteratively registering the slice sequence until no change is observed.

We assume that the registration reestablishes the original geometry of the slices, especially because it is restricted by the landmarks. Therefore we deform the first image with its initial dense deformation field, to correct its geometry such that the landmarks lie on the trajectories, as requested. The resulting slice is then used as reference image in the described non-rigid registration approach. The following slice is the template image. Its dense deformation field - the correction of its landmark positions to the fitted polynomials - serves as initialization for the non-rigid registration. This registration scheme is repeated throughout the entire data set.

To summarize, our proposed 3-D histological image reconstruction consists of the following steps, . also fig.3:

1. Selection of the landmarks on each slice
2. Fitting of polynomials to create volume trajectories
3. Creation of sparse deformation fields from the offsets of the landmarks to the polynomials
4. Transformation into a dense deformation field
5. Solving of the non-rigid registration problem.

3. Results

We tested our approach on two data sets. First, we created a synthetic image sequence comprised of a white disk with changing diameter and position representing a diagonal structure, and two white rectangles with fixed position on black background.

The second data set is a histological data set consisting of 350 Nissl-stained cryo sections of an adult mouse brain, available online by Ju et al [JWC*06]. For a typical slice example including the selected landmarks see fig. 4. For our reconstructions we selected the first 100 images of the mouse brain data set, as they show the main part of the structures in the brain. The image intensities were normalized and the slices rigidly registered beforehand.

We compare our method with a standard non-rigid registration scheme without landmarks, that is, without the Dirichlet boundary conditions. The amount of regularization for both methods is chosen such that the resulting images are deformed in a realistic manner without strong unnatural distortions, and to avoid the banana problem. These parameter settings were selected once and not changed for all experiments with both the synthetic and the histology images.

The first image is used as reference, and the subsequent images are matched to their respective already registered and warped predecessing slice.

Fig. 5 shows the results for the synthetic data set. The left image shows the original synthetic structure from the

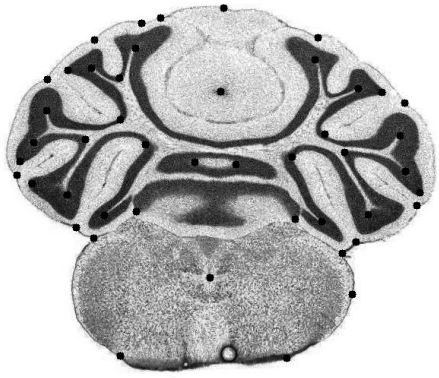

Figure 4: *A typical histological slice image with dots indicating selected landmarks.*

stacked images. The middle image was created by registering a slice with its already registered and deformed predecessor. Although the amount of regularization was rather high, the circular structure is almost entirely matched throughout the volume. This deformation also affects the shape of the white boxes, which originally should not change.

The reconstruction to the right shows the result of our approach, incorporating landmarks. Very slight changes are observable for the surfaces of the box structures. Otherwise their size and position remains preserved. Note again that the parameters settings were the same for both experiments. The only difference is the incorporation of the landmarks. Figure 6 shows exemplary instances of deformation fields. Here, higher intensities refer to higher deformation.

Fig.7 gives an overall impression of the reconstruction results of the histological data set.

As expected, the rigidly registered volume in the top row shows jagged contours and distortions of the slices. Using the standard non-rigid registration scheme, shown in the middle row, the contours are for the most part well matched. However, two problems are immediately noticeable. First, parts that appear to be curved in the rigidly registered volume are deformed such that they are for the greatest part stacked straight over each other. This is an example for the banana problem as described before. Second, the volume shows distinct blocks. After a number of slices where the contours are matched very well, there are strong jumps disrupting the spatial coherence of the structures.

The reason for the block effect is basically the application scheme of the non-rigid registration. The slices are deformed, and subsequently used as reference slice for the next section. In this case, the deformation of a certain structure might increase from slice to slice as it is matched against its counterpart in the already warped reference image.

There are two possible explanations of the result. First,

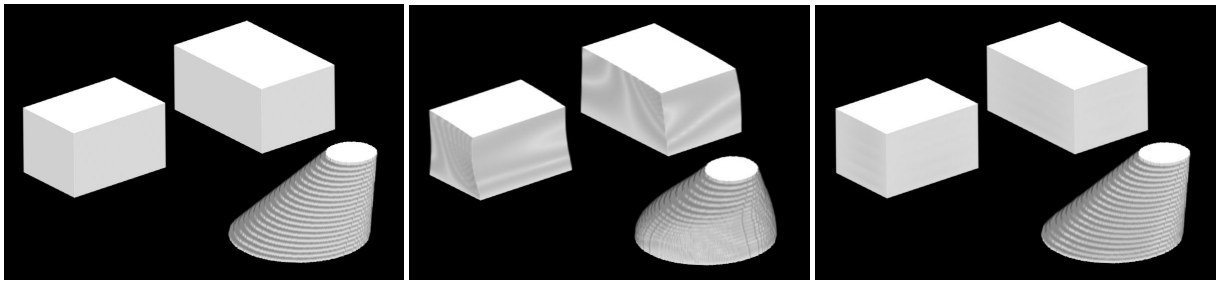

Figure 5: *Left: Original slices stacked as volume. Middle: Non-rigid registration without landmarks. Right: Improved reconstruction using the proposed approach with landmarks.*

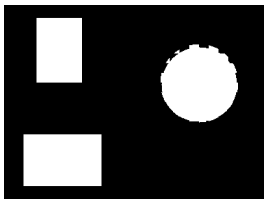

(a) Checkerboard image of reference and template images

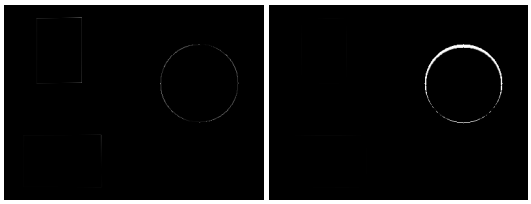

(b) Subtraction images after non-rigid registration

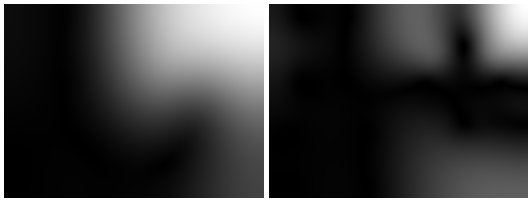

(c) Deformation images after registration

Figure 6: *Left column: Non-rigid registration without landmarks. Right column: Our approach. Note that the intensities of the deformation images are scaled for better visualization.*

it is possible that the structures of the template image are matched to different structures of the reference, that are dislocated due to the strong deformations. Basically, the optimization routine becomes trapped in a local minimum. A second possibility is that the regularization does not allow the amount of deformation that would be necessary to match the corresponding structures, and the registration stops some way in between. Both processes result in the observed jumps within the volume.

The last row of fig.7 shows the results using our proposed reconstruction method. Overall, the contours are much smoother compared to the rigidly registered volume. At the same time, the round shape of the brain and the curvature of the structures therein remains intact. This shows that the incorporation of the landmarks was able to prevent the straightening of the contours. Smoothing of the contours for a natural progression was however possible.

While the overall goal was achieved, there are still some problems present. Figure 8 shows a detail image of the reconstruction. While the effect is much less severe than in the normal non-rigid registration scheme described before, some jumps and straightened objects occur at some locations where no landmarks were set. As before, this can be considered to be mainly a cause of the successive increase of the deformations via the resampled reference images.

4. Discussion

Histological image reconstruction in the absence of ground truth data is about finding a balance between preservation of morphological correctness and the reestablishment of smooth and natural contours. Solely regularizing the deformation might not always be enough to prevent unnatural changes. The application of our method on one histological data set is certainly not enough to prove its efficiency and general applicability. But this article still gives a first impression about the potential of introducing landmarks into histological reconstructions as proposed in this work.

While a polynomial function was flexible enough to fit the structures of the data set used for the experiments, they might be too restrictive for more complicated, and especially longer structures. In this case other $\mathcal{C}^2$-continuous functions that are better able to follow these structures, e.g., B-Splines, should be used. Manual landmark extraction can be tedious and is prone to error. As the selected landmarks are forced onto the trajectories, inaccurate landmark positions exceeding small deviations might lead to problems.

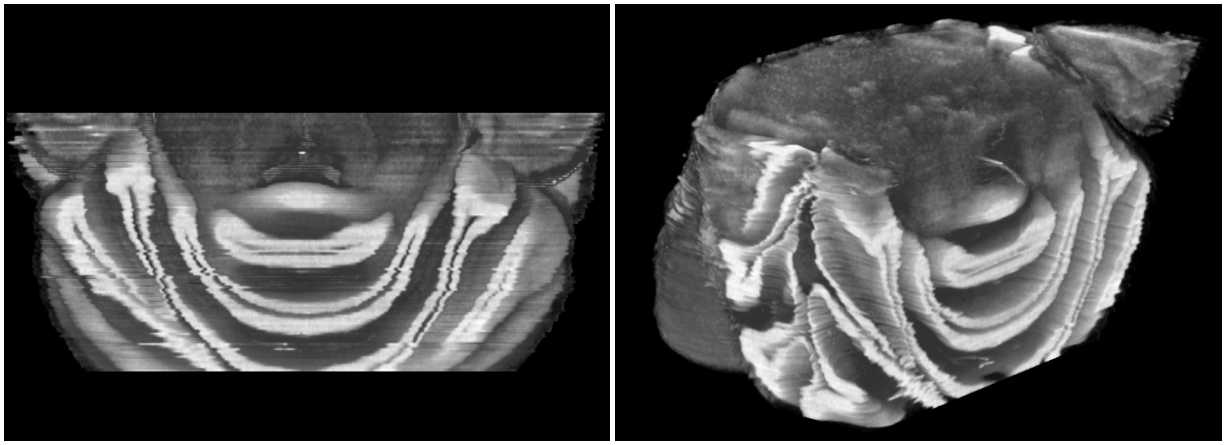

(a) Rigid registration

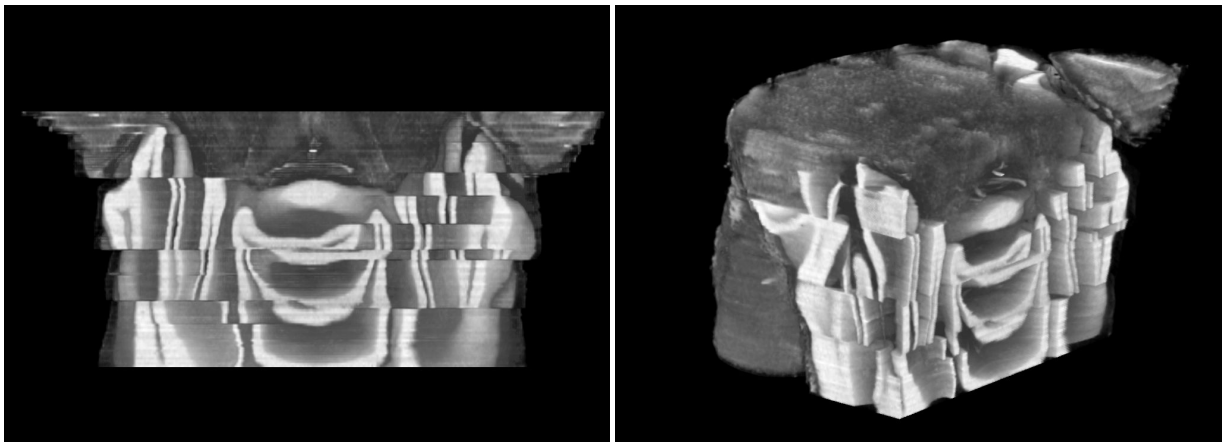

(b) Non-rigid registration without landmarks

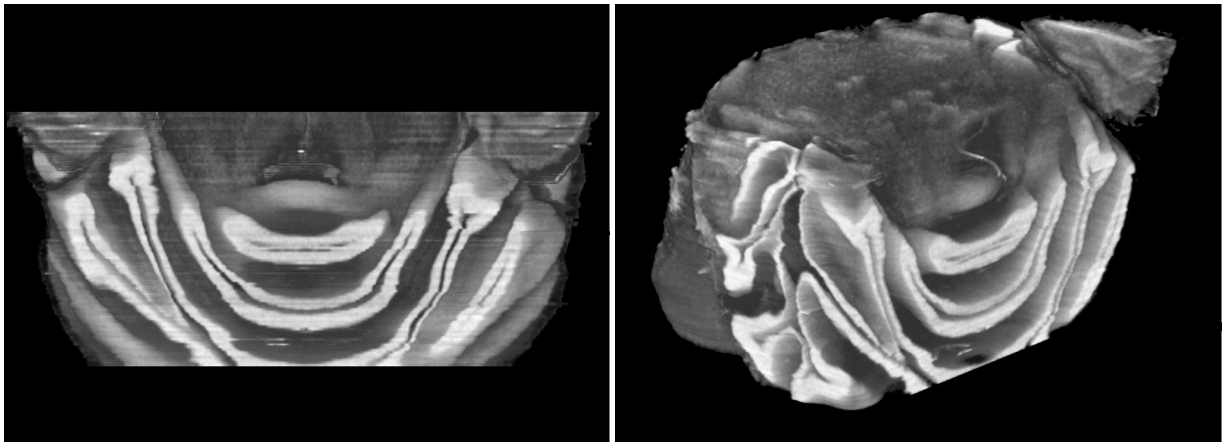

(c) Non-rigid registration with landmarks

Figure 7: *First row: Data set reconstructed by stacking rigidly registered slices. Middle row: Non-rigid registration without landmarks. Bottom: Improved reconstruction using the proposed approach with landmarks and the novel registration scheme.*

Therefore, reliable automatic landmark detection and tracking should be implemented. The complete distribution of the landmarks covering prominent anatomical features in the volume should be provided to prevent jumps. Furthermore, different application schemes of non-rigid registration of the image sequences should be investigated.

Finally, the applicability and benefit of our method for different types of histological data sets has to be investigated. The quality has to be objectively evaluated using ground truth data, and our approach has to be thoroughly compared to other methods in this field.

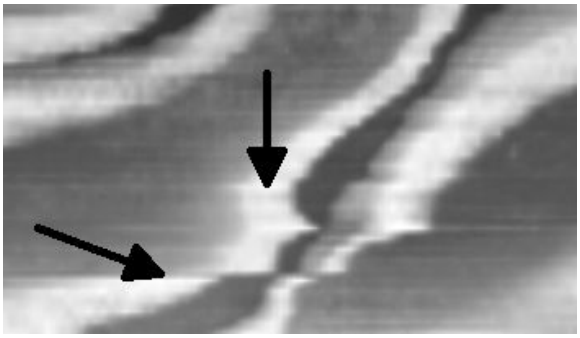

Figure 8: *Left arrow: Jump in reconstruction. Top arrow: Straightening of curve.*

Contribution

To conclude, we will sum up the main contributions of our work. First, we propose to explicitly distinguish between morphology-based offsets and artificially introduced warps. Instead of direct correspondences, we use landmarks to generate a morphology model, by fitting smooth polynomials approximating the original tissue sample. Dense deformation fields generated from this model serve as input into a non-rigid registration scheme. In our method, the landmarks are introduced as constraints in the registration formulation such that the optimization problem gets simpler with a growing number of landmarks. The algorithm can guarantee that the landmarks exactly match, which we use to relocate the landmarks to their approximated original location. The results show that our approach can efficiently smooth contours while preserving the morphological structure. It provides an additional means to preserve morphology in cases where normal methods would fail.

Acknowledgments

We thank Ju et al. [JWC*06] for providing the histological data set online. The authors gratefully acknowledge funding of the Erlangen Graduate School in Advanced Optical Technologies (SAOT) by the German National Science Foundation (DFG) in the framework of the excellence initiative. This work was supported by the Bundesministerium für Bildung und Forschung (BMBF), Germany (MoBiMed subproject 01EZ0807).

References

[DDC*07] DAUGUET J., DELZESCAUX T., CONDÉ F., MANGIN J., AYACHE N., HANTRAYE P., FROUIN V.: Three-dimensional reconstruction of stained histological slices and 3D non-linear registration with in-vivo MRI for whole baboon brain. *Journal of Neuroscience Methods 164*, 1 (Aug. 2007), 191–204. 2

[FM03a] FISCHER B., MODERSITZKI J.: Combining landmark and intensity driven registrations. *Proceedings in Applied Mathematics and Mechanics 3*, 1 (2003), 32–35. 2, 4

[FM03b] FISCHER B., MODERSITZKI J.: Curvature based image registration. *Journal of Mathematical Imaging and Vision 18*, 1 (2003), 81–85. 3

[HHC*02] HARTKENS T., HILL D. L. G., CASTELLANO-SMITH A. D., HAWKES D. J., MAURER C. R., MARTIN A. J., HALL W. A., LIU H., TRUWIT C. L.: Using points and surfaces to improve Voxel-Based non-rigid registration. In *Medical Image Computing and Computer-Assisted Intervention MICCAI 2002*, Dohi T., Kikinis R., (Eds.), vol. 2489. Springer Berlin Heidelberg, Berlin, Heidelberg, 2002, pp. 565–572. 2

[JC02] JOHNSON H. J., CHRISTENSEN G. E.: Consistent landmark and intensity-based image registration. *IEEE Transactions on Medical Imaging 21*, 5 (May 2002), 450–461. 2

[JWC*06] JU T., WARREN J., CARSON J., BELLO M., KAKADIARIS I., CHIU W., THALLER C., EICHELE G.: 3D volume reconstruction of a mouse brain from histological sections using warp filtering. *Journal of Neuroscience Methods 156*, 1-2 (Sept. 2006), 84–100. 2, 5, 8

[MEBNV04] MALANDAIN G., ÉRIC BARDINET, NELISSEN K., VANDUFFEL W.: Fusion of autoradiographs with an MR volume using 2-D and 3-D linear transformations. *NeuroImage 23*, 1 (Sept. 2004), 111–127. 2

[Mod03] MODERSITZKI J.: *Numerical Methods for Image Registration*. Oxford University Press, Dec. 2003. 2, 3

[PTVF07] PRESS W. H., TEUKOLSKY S. A., VETTERLING W. T., FLANNERY B. P.: *Numerical Recipes 3rd Edition: The Art of Scientific Computing*, 3 ed. Cambridge University Press, New York, NY, USA, 2007. 3

[SMH*07] SCHMITT O., MODERSITZKI J., HELDMANN S., WIRTZ S., FISCHER B.: Image registration of sectioned brains. *International Journal of Computer Vision 73*, 1 (June 2007), 5–39. 2

[SWM97] STREICHER J., WENINGER W. J., MÜLLER G. B.: External marker-based automatic congruencing: A new method of 3D reconstruction from serial sections. *The Anatomical Record 248*, 4 (1997), 583–602. 2

[UZDB06] URSCHLER M., ZACH C., DITT H., BISCHOF H.: Automatic point landmark matching for regularizing nonlinear intensity registration: Application to thoracic CT images. In *Medical Image Computing and Computer-Assisted Intervention MICCAI 2006*, Larsen R., Nielsen M., Sporring J., (Eds.), vol. 4191. Springer Berlin Heidelberg, Berlin, Heidelberg, 2006, pp. 710–717. 2